Asian Journal of Chemistry; Vol. 34, No. 2 (2022), 279-283

ASIAN JOURNAL OF CHEMISTRY

https://doi.org/10.14233/ajchem.2022.23470

Structural and Optical Properties of Chemically Deposited Metal Chalcogenide Thin Film CrS and its Photovoltaic Application

J. CHANDRASEKAR[1,2] and DURGACHALAM MANIKANDAN[2,*]

[1]Department of Physics, Tirukkoilur College of Arts and Science, Tirukkoilur-605766, India
[2]Department of Physics, Arignar Anna Government Arts College, Villupuram-605602, India

*Corresponding author: E-mail: a_dmani@yahoo.com

Received: 10 August 2021; *Accepted*: 28 September 2021; *Published online*: 11 January 2022; AJC-20648

In this work, chromium sulfide (CrS) thin films were grown on the acetic acid substrates by chemical bath deposition to prepare non-toxic photovoltaic devices. The combined single-source precursor approach has been developed for the deposition method using *tris*(diethyldithiocarbamato)chromium(III) for the deposition of CrS thin films grown at bath temperatures of 30, 60 and 90 ºC and at a constant deposition time of 30-120 min. The sufrace mophology of the prepared films have been analyzed by SEM and HR-TEM techniques. The study of the films indicate the distributed roughness and nano bundled hexagonal structures. The energy dispersive X-ray (EDX) spectroscopy analysis conformed the presence of Cr and S. The polycrystalline behaviour of the films was studied by an XRD study which revealed the mixed phases with a predicted crystallite size of 20 nm. The optical measurements showed films had a maximum transmittance of 90% in the visible region and the evaluated energy band varied in the range of 2.2-2.378 eV with the change of bath temperatures. This suggests that CrS thin film prepared at 90 ºC has enhanced crystalline superiority. According to photoluminescence (PL) analysis, the green emission can be attributed to the presence of several deep trap states or defects in the CrS structure. Moreover, natural dye sensitized solar cells (DSSCs) in CrS thin film prepared at 90 ºC, J_{sc} (28.0 mA/cm^2) produced a larger voltage in the short circuit as compared to synthetic dye sensitized solar cells (DSSCs) using CrS thin film J_{sc} (22.5 mA/cm^2).

Keywords: Surface morphology, Optical and electrical, Synthetic and natural based dye, Photovoltaic application.

INTRODUCTION

At present in the sphere of electro-optic technology, metal chalcogenide nanocrystalline solid thin film materials have started a new research field. Controlling the size and size distribution of semiconductor nanocrystallites is crucial in both basic and certain uses in photo electrochemical (PEC) and photovoltaic (PV) cells, dry electrodes for batteries, gas sensors, catalytic activity, laser applications and they are also frequently employed as a dry lubricant in electrical devices, which has sparked an interest in technological study [1-7]. These are shown as well as a variety of additional uses [8,9] as photocatalysts for dye degradation [10] and water splitting [11]. Chemical stability, a large energy band gap and controlled electrical characteristics are the key reasons for this [12]. The crystals were often loose and the films were often separated from the substrate [13].

Metal chalcogenide thin films can be made in a variety of ways, but chemical bath deposition is appealing since it requires simple and inexpensive machinery and scalable [14-18]. Because of their tunable structural and optical properties, diodes, solar selective coatings [19,20] and solar cell fabrication [21-24] are gaining popularity. Metal chalcogenide is a n-type semiconductor in the III-VI group of elements. It exists in various crystallographic phases depending on the synthesis, temperature and pressure and among these stages are: β-metal chalcogenide is the majority stable phase at room temperature [25]. The deposition of securely connected tightly packed nanocrystalline CrS sheets with tunable electrical, optical and physical properties for use in solar cells. As a result, an attempt is made in present study to deposit CrS layers employing *tris*-(diethyldithiocarbamato)chromium(III) as chromium precursor and acetic acid as a new complexing agent. The chemical and physical properties of the layers were examined after produced

by altering the composition. Moreover, the chemical deposition parameters affect carrier concentration, mobility and film thickness were also examined by altering the composition.

EXPERIMENTAL

The chemicals used in this study were *tris*(diethyldithiocarbamato)chromium(III), glacial acetic acid, HCl, ITO-coated glass, ruthenium dye, *Punica granatum* (pomegranate) fruit extract, deionized and ethanol. All the chemicals were procured from Sigma-Aldrich and used as such. Throughout the studies, glassware that had been cleansed with chromic acid and then carefully washed with distilled water.

The CrS was synthesized as thin films by chemical bath deposition technique (CBD) at different temperatures is a way of analyzing thin films. The precursor solutions were made by dissolving an accurate amount of *tris*(diethyldithiocarbamato)-chromium(III) in deionizer water, 3 drops of glacial acetic acid dissolved in ethanol in order to prevent precipitation and then added the optimized amount of HCl. It regulates pH levels between 1 and 4. The substrates were inserted vertically into the aqueous solution bath which was mounted on a heated magnetic agitator which controlled the solution's temperature and homogeneity. The CrS thin films were developed at bath temperatures of 30, 60 and 90 ºC for 120 min at a constant deposition time. After deposition, the thin films were cleaned in an ultrasonic bath for 10 min with deionized water. After deposition, the samples were allowed to cool naturally to room temperature. To determine the phases in films, XRD analysis was used. The study analyzed the morphological analysis, optical transmission and band gaps of several materials at different temperatures of 30, 60 and 90 ºC.

Characterization: An X-ray diffractometer (Bruker AXS D8) was used to investigate the structural characteristics of the materials utilizing Cu*K*α radiation of wavelength 1.5405 Å as the source. Properties of light A Varian Carry 5000 UV-Vis-NIR spectrophotometer was used to measure optical parameters such as absorption and transmission spectra in the 200-2000 nm region. A Carl Zeiss EVO MA 15 scanning electron microscope was used to examine the surface morphology and grain size of the films.

RESULTS AND DISCUSSION

SEM studies: The grains were homogeneously distributed as the formed film surface was made up of small particles which cover the whole uniform distribution. The cubic crystal roughness in the region of 10 μm is shown in Fig. 1a. The EDS spectrum presence of Cr and S in CrS thin films is shown in Fig. 1b.

HR-TEM studies: Transmission electron microscopy (TEM) images of the samples results in mean diameters of the CrS of 20 nm. At 90 °C, the film contaied a nano bundle hexagonal shaped structure (Fig. 2a). The number of diffraction strong rings was visible in the SAED-selected area electron diffraction sequence, which correlates with different crystal planes of the polycrystalline nature of thin film (Fig. 2b-c). Fig. 2d represents an 3D surface image of thin film structure whereas, Fig. 2e shows the average particle size was 228.1 nm. The individual particle as shown in Fig. 2a revealed that most of the particles are elongated. However, a slight aggregation of particles has been observed in pure samples of thin film. It is observed that inspite of the agglomeration of nanoparticles, they contain a narrow size distribution.

Structural properties: Fig. 3a-c show the film's characteristic nature with the heterogeneous phases. The thin film correlates to the configurations of (002), (130), (110), (332) and (220) and refers to cubic structure of chromium sulfide as per standard JCPDS data card no. [81-0105, 73-0844]. The XRD peak results likely same d-value of orientation at 30 ºC (Fig. 3a) where a very lowest peak appear, at 60 ºC, a lowest sharp peak appear (Fig. 3b), while at 90 ºC (Fig. 3c), a highest sharp peak appeared from the same θ value of thin films. According to Debye Scherrer's calculation for CrS thin films at 30, 60 and 90 ºC, the grain size was 23, 21 and 17 nm, respectively. The reduction in crystallite size in thin films at high temperature is due to an increase in the nucleation region density.

Optical studies: The optical properties of the CrS thin films in the optical and near-infrared regions in the wavelength range of 300-1200 nm exhibit good transmission. Due to the obvious irregularity of the films, average transmittance was expanded significantly to 90% on 30 ºC thin film with an incre-

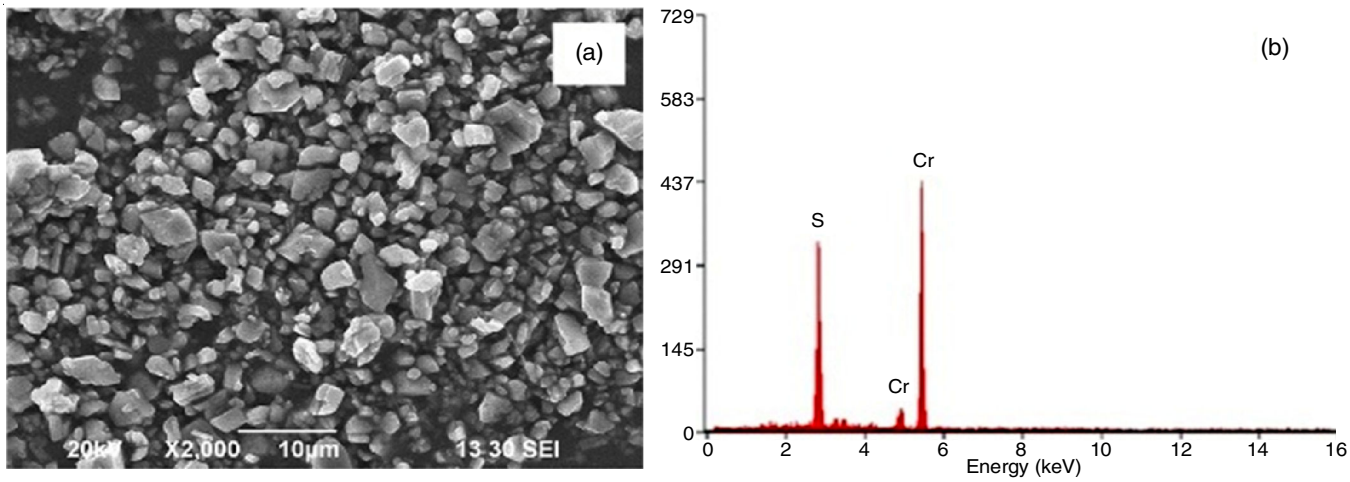

Fig. 1. HR-SEM analysis (a) SEM image of CrS thin film and (b) EDS analysis

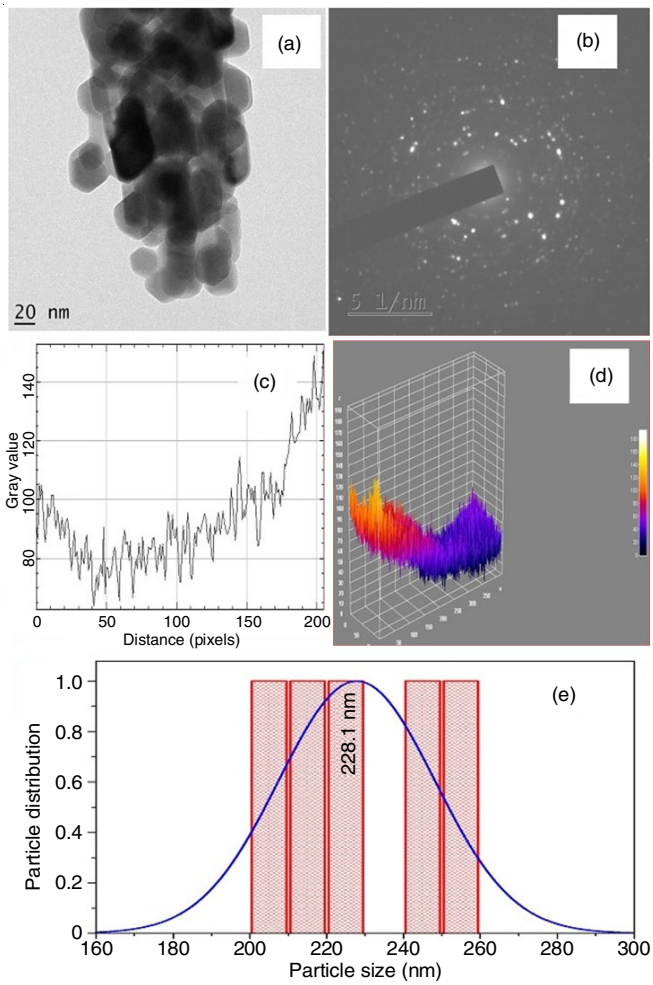

Fig. 2. HR-TEM analysis of (a) image InS thin film, (b) SAED pattern, (c) Plot profile, (d) interactive 3D-surface plot spectrum and (e) size in a specific area figure that has been emphasised (a) a really thin film

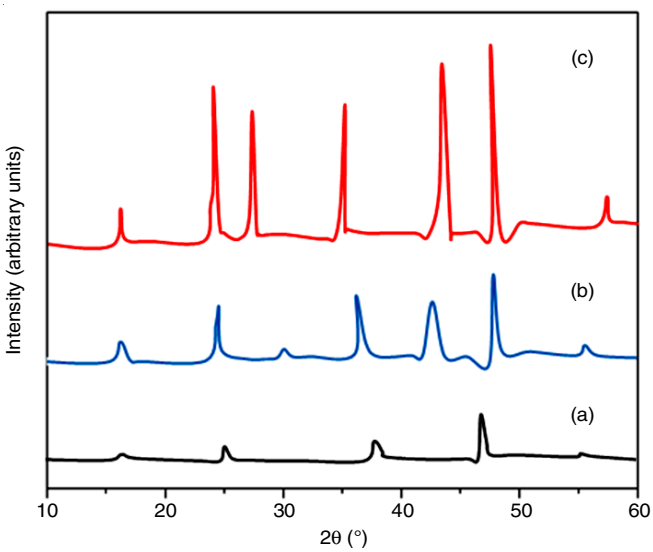

Fig. 3. XRD spectra of the CrS thin films grown at various bath temperatures (a) 30 ºC, (b) 60 ºC and (c) 90 ºC by chromium sulfide thin films

asing bath temperature of 90 ºC, indicating excellent transmittance (Fig. 4a-c). The strength of the films may be results

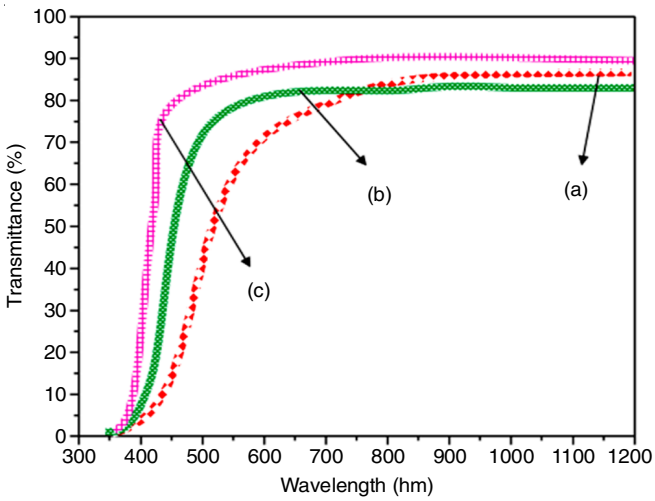

Fig. 4. Transmittance at various bath temperatures (a) 30 °C, (b) 60 °C and (c) 90 °C by chromium sulfide thin films

in the improvement in transmittance. A high degree of transparency is linked to structural homogeneity and polycrystalline structure. As a result, the thin film prepared at 90 ºC is appropriate for clear conductive films. The film's greater transparency in the visible range indicates its possible use in solar technology applications than that of lower temperature CrS thin film [18]. The relative amid the combination coefficients -αhν and photon energy –hν for direct transition

$$\alpha h\nu = A(h\nu - E_g)^n$$

while A is a constant; E_g is the band gap frequency and denotes the quantity which affects the quality of the transition for direct and indirect transitions correspondingly for 1/2 and 2. Fig. 5a-c illustrates typical $(h\nu)^2$ against hν plots. The increased carrier temperature causes the optical band gap to shrink to 2.2-2.378 eV with increasing high temperature film content. Similar results were observed when the novelist claims that rising mover focus causes band shrinkage and shifts in optical band gaps [26]. The reduction in band gap of 90 ºC (CrS) thin films compared to 60 ºC and 30 ºC (CrS) thin films is due to changes in film solidity and grain extent.

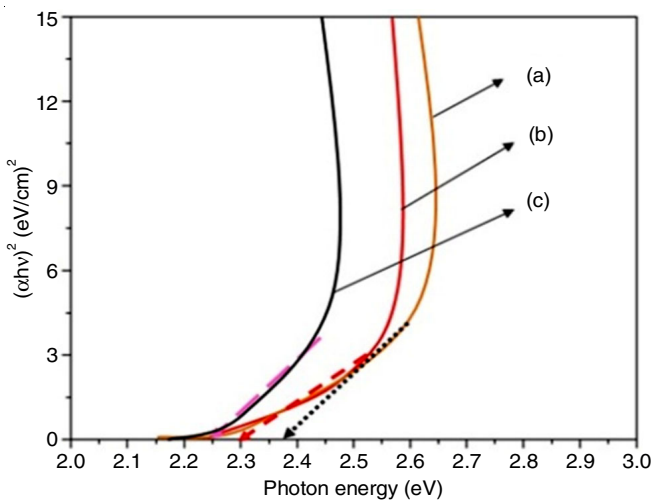

Fig. 5. $(\alpha h\nu)^2$ *versus* photon energy of plots; chromium sulfide thin films grown various bath temperatures (a) 30 ºC, (b) 60 ºC and (c) 90 ºC

Extinction coefficient: In the characterization using the relationship between refractive directory is computed for various wavelengths is calculated by $n = \frac{1+R^{1/2}}{1-R^{1/2}}$. In this study, the rise in reflectance with rising temperatures could be linked to an increase in the clean compactness of the films, which lowers the temperature component of the films. As the temperature rises, the average value of the refractive index of CrS thin film prepared at 90 ºC decreases (Fig. 6a-c). It is possible that the film's optical density has been decreased as a result of the high temperature thin coating.

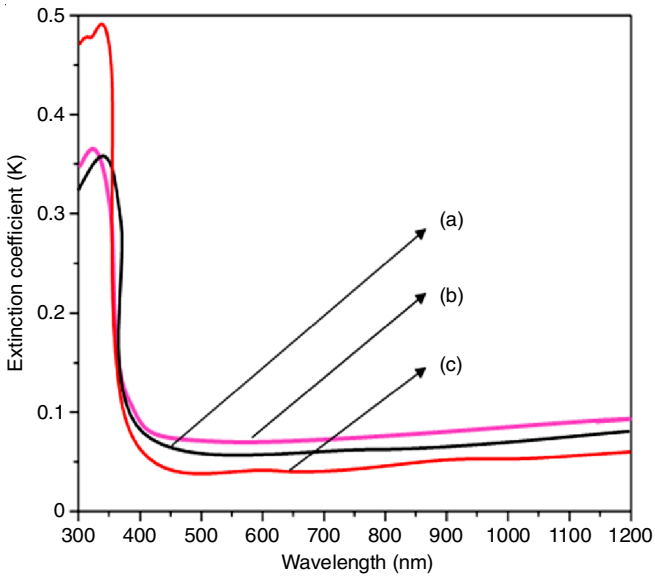

Fig. 6. Extinction coefficient of grown various bath temperatures (a) 30 ºC, (b) 60 ºC and (c) 90 ºC of chromium sulfide thin films

Photoluminescence: The CrS films have two emission signals at ambient temperature, one centred between 2.2-2.3782 eV and the other at 2.4 eV. The green fluorescence (2.2-2.3782 eV) could be due to chromium interstial sites. The CrS samples are red-shifted in relation to the substrate emission the CrS thin film at prepared at 30 ºC exhibited the emission at 2.2 eV, the CrS thin film at prepared at 60 ºC has the signal centred at 2.3 eV, while the CrS thin film at prepared at 90 ºC has the signal centred at 2.2 eV (Fig. 7a-c). A decrease in the band gap energy increases the intensity of CrS thin film prepared at high temperature (90 ºC) results in the improvement of crystallinity [27].

Photovoltaic applications

Synthetic dye based DSSCs: The chromium sulfide acts as a photo electrode and is deposited on FTO-plate glass at temperatures ranging from 30 to 90 ºC. Thin films containing synthetic dye (ruthenium dye, 535-bisTBA, N719) were used to make the solar cell. The CrS thin film prepared at 90 ºC using dye as a sensitizer exhibits the greatest values of J_{sc} (22.5 mA/cm^2 (Fig. 8a-c), open-circuit voltage V_{oc} (500 mV), fill factor FF (0.94) and productivity g (1.7%) as compared to CrS (a) 30 ºC and (b) 60 ºC thin film J_{sc} (15.9 and 17 mA/cm [28,29].

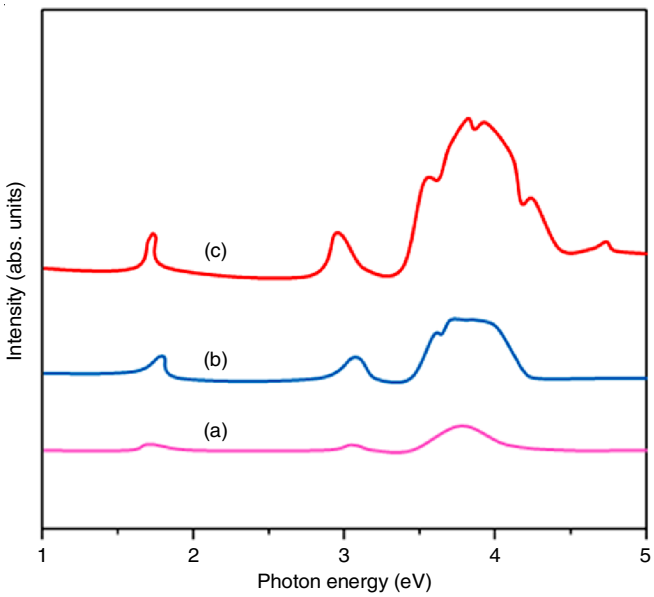

Fig. 7. Photoluminescence of grown various bath temperatures (a) 30 ºC, (b) 60 ºC and (c) 90 ºC of chromium sulfide thin films

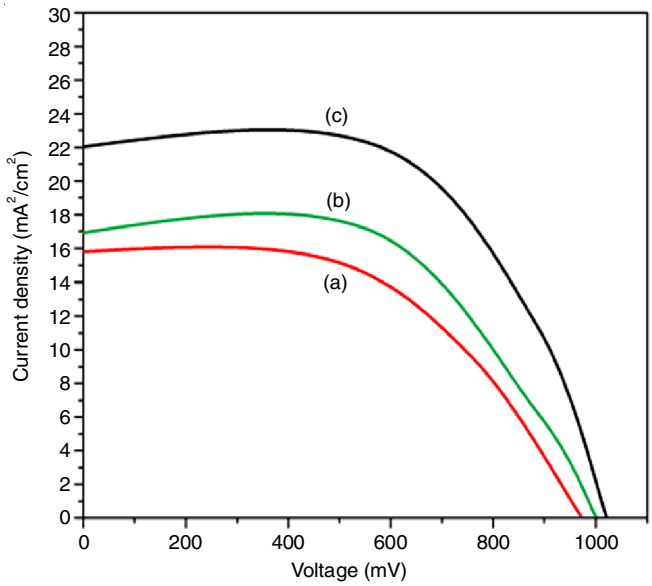

Fig. 8. Current density voltage [J-V] curves for the DSSC's fabricated from (a) CrS- 30 ºC film coated GCE, (b) CrS- 60 ºC film GCE and (c) (b) CrS- 90 ºC film GCE by synthetic dye

Natural dye based DSSCs: Chromium sulfide acts as a photo-electrode and is deposited on FTO-plate glass at temperatures ranging from grown at various bath temperatures by CrS thin films containing natural dye for *Punica granatum* (pomegranate) fruit extract form was employed to make the solar cell. The CrS thin film prepared at 90 ºC using natural dye as a sensitizer exhibit the greatest values of J_{sc} (28.0 mA/cm^2), V_{oc} (500 mV), fill factor, FF (0.94) and productivity, g (1.7%) that of CrS (a) 30 ºC and (b) 60 ºC thin film J_{sc} (23.8 and 25 mA/cm^2) (Fig. 9a-c) [30]. As a result, natural dye sensitized solar cells (DSSCs) in CrS thin film prepared at 90 ºC, J_{sc} (28.0 mA/cm^2) produced a larger voltage in the short circuit as compared to synthetic dye sensitized solar cells (DSSCs) using CrS thin film J_{sc} (22.5 mA/cm^2).

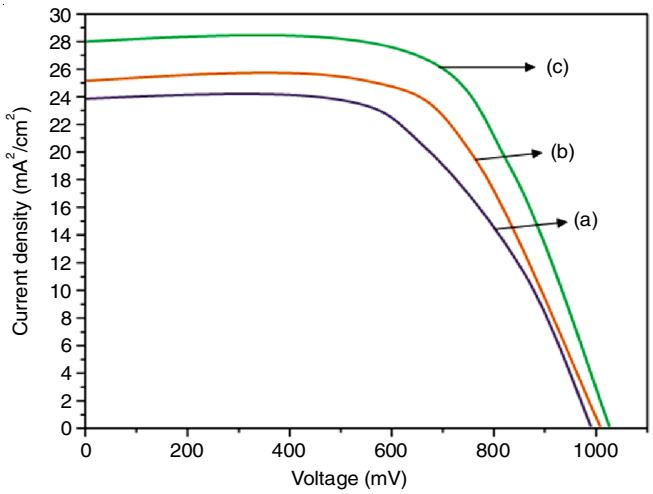

Fig. 9. Current density voltage [J-V] curves for the DSSC's fabricated from (a) CrS- 30 ºC film coated GCE, (b) CrS- 60 ºC film GCE and (c) (b) CrS- 90 ºC film GCE by natural dye

Conclusion

The structural and optical properties of chemically deposited chromium sulfide thin films were deposited on acetic acid substrates by chemical bath deposition at different temperatures 30-90 ºC. The characterization of SEM and HRTEM The study of the films also distributed roughness and nano bundle hexagonal shaped structures and the number of diffraction strong rings were visible in the SAED-pattern correlates as different crystal planes of polycrystalline nature. The EDS spectrum results confirmed the presence of thin film percent. The XRD results show that the reduction in crystallite size in thin films at high temperatures is due to an increase in nucleation region density. The chromium sulfide films grown at CrS-60 ºC and CrS-90 ºC have the highest transmittance in the visible region; between 82% and 90%. This makes CrS films grown by chemical bath deposition at 90 ºC potentially reliable for flexible photovoltaic applications. It can be established that natural dye sensitized solar cells (DSSCs) have a higher current generated in the shat circuit than synthesized dye sensitized solar cells for photovoltaic applications, respectively.

CONFLICT OF INTEREST

The authors declare that there is no conflict of interests regarding the publication of this article.

REFERENCES

1. P.K. Kannan, D.J. Late, H. Morgan and C.S. Rout, *Nanoscale*, **7**, 13293 (2015); https://doi.org/10.1039/C5NR03633J
2. T.F. Jaramillo, K.P. Jørgensen, J. Bonde, J.H. Nielsen, S. Horch and I. Chorkendorff, *Science*, **317**, 100 (2007); https://doi.org/10.1126/science.1141483
3. J.-H. Cha, S.-J. Choi, S. Yu and I.-D. Kim, *J. Mater. Chem. A Mater. Energy Sustain.*, **5**, 8725 (2017); https://doi.org/10.1039/C6TA11019C
4. D.J. Lewis, A.A. Tedstone, X.L. Zhong, E.A. Lewis, A. Rooney, N. Savjani, J.R. Brent, S.J. Haigh, M.G. Burke, C.A. Muryn, J.M. Raftery, C. Warrens, K. West, S. Gaemers and P. O'Brien, *Chem. Mater.*, **27**, 1367 (2015); https://doi.org/10.1021/cm504532w
5. Y. Xu, E. Hu, K. Hu, Y. Xu and X. Hu, *Tribol. Int.*, **92**, 172 (2015); https://doi.org/10.1016/j.triboint.2015.06.011
6. A.M. Malyarevich, M.S. Gaponenko, V.G. Savitski, K.V. Yumashev, G.E. Rachkovskaya and G.B. Zakharevich, *J. Non-Cryst. Solids*, **353**, 1195 (2007); https://doi.org/10.1016/j.jnoncrysol.2007.01.018
7. Y. Sang, Z. Zhao, M. Zhao, P. Hao, Y. Leng and H. Liu, *Adv. Mater.*, **27**, 363 (2015); https://doi.org/10.1002/adma.201403264
8. V. Stancu, E. Pentia, A. Goldenblum, M. Buda, G. Iordache and T. Botila, *Rom. J. Inf. Sci. Technol.*, **10**, 53 (2007).
9. W. Chen, J.-O. Bovin, A.G. Joly, S. Wang, F. Su and G. Li, *J. Phys. Chem. B*, **108**, 11927 (2004); https://doi.org/10.1021/jp048107m
10. Y. He, D. Li, G. Xiao, W. Chen, Y. Chen, M. Sun, H. Huang and X. Fu, *J. Phys. Chem. C*, **113**, 5254 (2009); https://doi.org/10.1021/jp809028y
11. X. Fu, X. Wang, Z. Chen, Z. Zhang, Z. Li, D.Y.C. Leung, L. Wu and X. Fu, *Appl. Catal. B*, **95**, 393 (2010); https://doi.org/10.1016/j.apcatb.2010.01.018
12. N. Barreau, S. Marsillac, J.C. Bernede and L. Assmann, *J. Appl. Phys.*, **93**, 5456 (2003); https://doi.org/10.1063/1.1565823
13. S. Seghaier, N. Kamoun, R. Brini and A.B. Amara, *Mater. Chem. Phys.*, **97**, 71 (2006); https://doi.org/10.1016/j.matchemphys.2005.07.061
14. G.R. Gopinath, R.W. Miles and K.T.R. Reddy, *Energy Procedia*, **34**, 399 (2013); https://doi.org/10.1016/j.egypro.2013.06.768
15. Z. Gao, J. Liu and H. Wang, *Mater. Sci. Semicond. Process.*, **15**, 187 (2012); https://doi.org/10.1016/j.mssp.2012.02.004
16. F. Trigo, B. Asenjo, J. Herrero and M.T. Gutiérrez, *Sol. Energy Mater. Sol. Cells*, **92**, 1145 (2008); https://doi.org/10.1016/j.solmat.2008.04.002
17. B. Yahmadi, N. Kamoun, C. Guasch and R. Bennaceur, *Mater. Chem. Phys.*, **127**, 239 (2011); https://doi.org/10.1016/j.matchemphys.2011.01.066
18. P.E. Rodríguez-Hernández, K.E. Nieto-Zepeda, A. Guillén-Cervantes, J. Santoyo Salazar, J. Santos-Cruz and J.S. Arias-Cerón, *Chalcogenide Lett.*, **14**, 331 (2017).
19. L. Luo, Y. Zhang, S.S. Mao and L. Lin, *Sens. Actuator A Phys.*, **127**, 201 (2006); https://doi.org/10.1016/j.sna.2005.06.023
20. P.K. Nair, V.M. Garcia, A.B. Hernandez and M.T.S. Nair, *J. Phys. D*, **24**, 1466 (1991); https://doi.org/10.1088/0022-3727/24/8/036
21. R.D. Engelken, H.E. McCloud, C. Lee, M. Slayton and H.J. Ghoreishi, *J. Electrochem. Soc.*, **134**, 2696 (1987); https://doi.org/10.1149/1.2100274
22. M. Jayachandran, M.J. Chokalingam and V.K. Venkatesan, *J. Mater. Sci. Lett.*, **8**, 563 (1989); https://doi.org/10.1007/BF00720299
23. B.A. Parkinson, A. Heller and B. Miller, *Appl. Phys. Lett.*, **33**, 521 (1978); https://doi.org/10.1063/1.90422
24. I. Gur, N.A. Fromer, M.L. Geier and A.P. Alivisatos, *Science*, **310**, 462 (2005); https://doi.org/10.1126/science.1117908
25. N. Barreau, *Sol. Energy*, **83**, 363 (2009); https://doi.org/10.1016/j.solener.2008.08.008
26. S. Ilican, Y. Caglar, M. Caglar and F. Yakuphanoglu, *Appl. Surf. Sci.*, **255**, 2353 (2008); https://doi.org/10.1016/j.apsusc.2008.07.111
27. Y. Xing, H. Zhang, S. Song, J. Feng, Y. Lei, L. Zhao and M. Li, *Chem. Commun.*, 1476 (2008); https://doi.org/10.1039/B717512D
28. J. Liu, H. Yang, W. Tan, X. Zhou and Y. Lin, *Electrochim. Acta*, **56**, 396 (2010); https://doi.org/10.1016/j.electacta.2010.08.063
29. Y. Zhang, L. Wang, B. Liu, J. Zhai, H. Fan, D. Wang, Y. Lin and T. Xie, *Electrochim. Acta*, **56**, 6517 (2011); https://doi.org/10.1016/j.electacta.2011.04.118
30. T.A. Ruhane, M.T. Islam, M.S. Rahaman, M.M.H. Bhuiyan, J.M.M. Islam, M.K. Newaz, K.A. Khan and M.A. Khan, *Optik*, **149**, 174 (2017); https://doi.org/10.1016/j.ijleo.2017.09.024